GEOLOGY | THE GEOLOGICAL SOCIETY OF AMERICA®

https://doi.org/10.1130/G46546.1

Manuscript received 22 May 2019
Revised manuscript received 11 October 2019
Manuscript accepted 21 October 2019

Published online 22 November 2019

Regional and global signals in seawater $\delta^{18}O$ records across the mid-Pleistocene transition

Heather L. Ford* and Maureen E. Raymo
Lamont-Doherty Earth Observatory, Columbia University, Palisades, New York 10964, USA

ABSTRACT

High-resolution seawater $\delta^{18}O$ records, derived from coupled Mg/Ca and benthic $\delta^{18}O$ analyses, can be used to evaluate how global ice volume changed during the mid-Pleistocene transition (MPT, ca. 1250–600 ka). However, such seawater $\delta^{18}O$ records are also influenced by regional hydrographic signals (i.e., salinity) and changes in deep-ocean circulation across the MPT, making it difficult to isolate the timing and magnitude of the global ice volume change. To explore regional and global patterns in seawater $\delta^{18}O$ records, we reconstruct seawater $\delta^{18}O$ from coupled Mg/Ca and $\delta^{18}O$ analyses of *Uvigerina* spp. at Ocean Drilling Program Site 1208 in the North Pacific Ocean. Comparison of individual seawater $\delta^{18}O$ records suggests that deep-ocean circulation reorganized and the formation properties (i.e., salinity) of deep-ocean water masses changed at ca. 900 ka, likely related to the transition to marine-based ice sheets in Antarctica. We also find that an increase in ice volume likely accompanied the shift in glacial-interglacial periodicity observed in benthic carbonate $\delta^{18}O$ across the MPT, with increases in ice volume observed during Marine Isotope Stages 22 and 16.

INTRODUCTION

Even after decades of research, the mid-Pleistocene transition (MPT) remains a perplexing interval in Earth's climate history (Shackleton and Opdyke, 1976; Raymo and Nisancioglu, 2003; Elderfield et al., 2012). A change from low-amplitude 41 k.y. glacial-interglacial cycles to larger-amplitude 100-k.y.-dominated glacial-interglacial cycles is observed in all foraminiferal $\delta^{18}O$ records (as well as many other climate proxy records), although the timing of this transition varies by location. Some records suggest that the MPT was gradual (Ruddiman et al., 1989; Clark et al., 2006; Sosdian and Rosenthal, 2009), whereas others show a more abrupt change (Mudelsee and Schulz, 1997; Elderfield et al., 2012). In the spectral domain, a weak 100 k.y. signal is observed in records of sea-surface temperature and $\delta^{18}O$ of benthic foraminifera ($\delta^{18}O_{benthic}$) as early as 1200 ka (Clark et al., 2006; McClymont et al., 2013). By Marine Isotope Stage (MIS) 22 (ca. 900 ka), the 100 k.y. cycle emerges as statistically significant, and at MIS 16 (ca. 600 ka), the transition is considered complete (Mudelsee and Schulz, 1997). Of course, all spectral methods are based on averaging a signal across a generally long time interval.

Another difficulty in evaluating the timing (and mechanisms) of the MPT is that $\delta^{18}O_{benthic}$ values, our primary climate proxy, reflect not just the $\delta^{18}O$ of seawater ($\delta^{18}O_{sw}$, salinity and ice volume), but also bottom-water temperature and the circulation history of the water mass over a particular location (Clark et al., 2006; Ford et al., 2016). High-latitude conditions imprint temperature and salinity properties on water-mass parcels that sink and ultimately traverse the ocean's depths (Talley, 2013). In polar regions, the salinity of sinking water masses is controlled by atmospheric processes (evaporation and precipitation), as well as by sea ice processes such as brine rejection (Brennan et al., 2013). To separate these effects, studies have used the Mg/Ca of benthic foraminifera to isolate the temperature contribution to $\delta^{18}O_{benthic}$ (Sosdian and Rosenthal, 2009; Elderfield et al., 2012). However, changes in ocean circulation remain a confounding factor because associated water-mass salinity variations can also influence these records (Ford et al., 2016).

Here we present a new Mg/Ca-derived $\delta^{18}O_{sw}$ reconstruction from Ocean Drilling Program (ODP) Site 1208 in the North Pacific Ocean (Fig. 1). This location is at the end of the "global conveyor belt" and sits within Pacific Deep Water (PDW). PDW is an old, well-mixed water mass primarily composed of Southern Component Water (SCW) (Talley, 2013) and is also the most voluminous water mass globally (Worthington, 1981). We compare and combine our record with previously published Mg/Ca-derived $\delta^{18}O_{sw}$ reconstructions from ODP Site 1123 in the South Pacific (41.8°S, 171.5°W, 3290 m water depth; Elderfield et al., 2012) and Deep Sea Drilling Project (DSDP) Site 607 in the North Atlantic Ocean (41.0°N, 33.0°W, 3427 m water depth; Sosdian and Rosenthal, 2009; Ford et al., 2016) to generate a $\delta^{18}O_{sw}$ stack. We show that deep-ocean circulation reorganization and salinity played an increasingly important role in determining the density structure of the glacial deep ocean over the MPT. With this first $\delta^{18}O_{sw}$ stack across the MPT, we are able to provide an estimate of changes in global ice volume across this important climate transition.

MATERIALS AND METHODS

ODP Site 1208 is a single-hole drilling location on Shatsky Rise (36.1°N, 158.2°E, 3346 m water depth). Sampling varies from 1.4 to 3.7 k.y. resolution. For oxygen isotope analyses, between two and four *Uvigerina* spp. shells were picked from the >250 µm size fraction of each sample and were analyzed on an Elementar Isoprime 100 stable isotope ratio mass spectrometer with dual inlet at Lamont-Doherty Earth Observatory (Palisades, New York, USA). Long-term precision is 0.06‰. Using the $\delta^{18}O_{benthic}$ record, an age model was generated using the HMM-Stack Matlab code (Lin et al., 2014; Butcher et al., 2017), which aligns to the Prob-stack (a probabilistic Pliocene–Pleistocene stack of benthic $\delta^{18}O$ using a profile hidden Markov model; Ahn et al., 2017). Prob-stack includes 180 $\delta^{18}O_{benthic}$ globally distributed records and is an updated version of the LR04 stack and time scale (Lisiecki and Raymo,

*Current address: School of Geography, Queen Mary University of London, London E1 4NS, UK

CITATION: Ford, H.L., and Raymo, M.E., 2020, Regional and global signals in seawater $\delta^{18}O$ records across the mid-Pleistocene transition: Geology, v. 48, p. 113–117, https://doi.org/10.1130/G46546.1

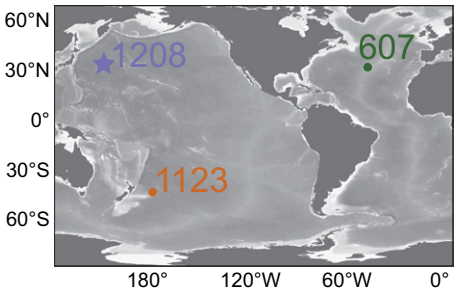

Figure 1. Location map for three core locations: Ocean Drilling Program (ODP) Site 1208 (this study), ODP Site 1123 (Elderfield et al., 2012), and Deep Sea Drilling Project (DSDP) Site 607 (Sosdian and Rosenthal, 2009; Ford et al., 2016).

2005). Prob-stack is similar in form to LR04 over the interval studied here.

For Mg/Ca analyses, between six and 12 *Uvigerina* spp. shells from each sample were analyzed on Thermo Scientific iCAP-Q inductively coupled plasma mass spectrometers (ICP-MS) at Lamont-Doherty Earth Observatory and at Rutgers University (New Jersey, USA) (see the GSA Data Repository[1]). Mg/Ca values were converted to bottom-water temperature (BWT) using a modified version of the *Uvigerina* spp. paleotemperature equation (Elderfield et al., 2010, 2012; Ford et al., 2016) to account for the reductive cleaning step used in this study.

The $\delta^{18}O_{benthic}$ and BWTs were then used to derive $\delta^{18}O_{sw}$ using PSU Solver computational toolkit, which uses Monte Carlo simulations to constrain uncertainty (Thirumalai et al., 2016). Our $\delta^{18}O_{sw}$ stack was generated by (1) interpolating each $\delta^{18}O_{sw}$ record to an even 3 k.y. interval (across the 338–1450 ka interval where all three records have ≤ 3 k.y. sample resolution), (2) bootstrapping the records to estimate error, and (3) averaging the interpolated means and bootstrapped error estimates (see the Data Repository). The age models for DSDP Site 607 and ODP Site 1123 were not modified because their age models were tied to LR04 and there is little difference between LR04 and Prob-stack in this interval.

RESULTS

The $\delta^{18}O_{benthic}$ record from ODP Site 1208 (Fig. 2B) is similar in trend and structure to Prob-stack (Fig. 2A). At Site 1208, there is a gradual increase in glacial $\delta^{18}O_{benthic}$ values from the early Pleistocene at ca. 1400 to ca. 600 ka when there is a stepped increase in $\delta^{18}O_{benthic}$ values at MIS 16. Glacial BWTs show near-freezing values over most the record in the North Pacific (Fig. 2C; see the Data Repository), similar to the South Pacific (Elderfield et al., 2012). However, at Site 1208, glacial MIS 22 shows a strong warming and ~1‰ transient increase in glacial $\delta^{18}O_{sw}$ values relative to the early MPT (Fig. 2D). The large $\delta^{18}O_{sw}$ increase at MIS 22 is not repeated in MIS 20 or MIS 18. We do not see changes in preservation or contamination that might affect our records (see the Data Repository). Because this positive $\delta^{18}O_{sw}$ excursion is associated with warm BWTs as indicated by the Mg/Ca data (Figs. 2C and 2D), this implies that either a large ice-volume growth event happened at MIS 22 and/or the warm bottom-water mass was also characterized by higher salinity.

THE "900 KA EVENT": OCEAN CIRCULATION, WATER MASSES, AND ANTARCTIC ICE-SHEET TRANSITION

The ODP Site 1208 and DSDP Site 607 $\delta^{18}O_{sw}$ histories are not consistent with Elderfield et al.'s (2012) conclusion that an abrupt, large increase in Antarctic ice volume occurred at MIS 22 and recurred during subsequent glacial periods, particularly MIS 20 and 18 (Figs. 3A–3C). The observation of a transient increase in $\delta^{18}O_{sw}$ at Site 1208 during MIS 22 (this study) and a gradual increase in $\delta^{18}O_{sw}$ throughout the MPT at Site 607 (Sosdian and Rosenthal, 2009; Ford et al., 2016) suggests that hydrographic changes also occurred over the MPT. In other words, if global ice volume grew during MIS 22 and persisted during subsequent glacials as Elderfield et al. (2012) suggested, the stepped glacial increase in $\delta^{18}O_{sw}$ observed at Site 1123 should certainly be present at both Pacific locations. However, the $\delta^{18}O_{sw}$ increase at MIS 22 is absent during the subsequent glacial MIS 20 and MIS 18 at Site 1208. As an alternative interpretation, we suggest that the $\delta^{18}O_{sw}$ increase at Site 1123 at MIS 22 and subsequent glacials can be attributed to changes in deep-ocean circulation, salinity stratification, *and* an increase global ice volume.

Neodymium (Pena and Goldstein, 2014) and carbon records (Raymo et al., 1997; Venz et al., 1999; Lisiecki, 2014; Lear et al., 2016; Farmer et al., 2019) show that Atlantic Northern Component Water (NCW) decreased in spatial extent ca. 900 ka. During the early Pleistocene, NCW dominated the intermediate and deep Atlantic basin during both glacials and interglacials (Pena and Goldstein, 2014). At the "900 ka event," during a time of anomalously low Southern Hemisphere insolation, Antarctic sea ice expanded and SCW flooded the South Atlantic at intermediate and deep ocean depths (Kemp et al., 2010; Pena and Goldstein, 2014). After MIS 22, carbon and neodymium isotopes show that NCW has been prominent during interglacials at intermediate and deep ocean depths, while SCW has dominated the deep ocean during glacials (Raymo et al., 1997; Pena and Goldstein, 2014).

What processes could have contributed to deep-ocean circulation and water-mass property changes at MIS 22? One possibility is that a transition from terrestrial to marine-based ice sheets in Antarctica (Raymo et al., 2006) around MIS 22 may have altered the distribution of deep-ocean water masses and water-mass properties in their formation areas. The transition from a largely terrestrial-based ice sheet to marine-based ice shelf would have also promoted the formation of coastal polynyas, like those in the Ross and Weddell Seas (Morales Maqueda et al., 2004), which increase salinity

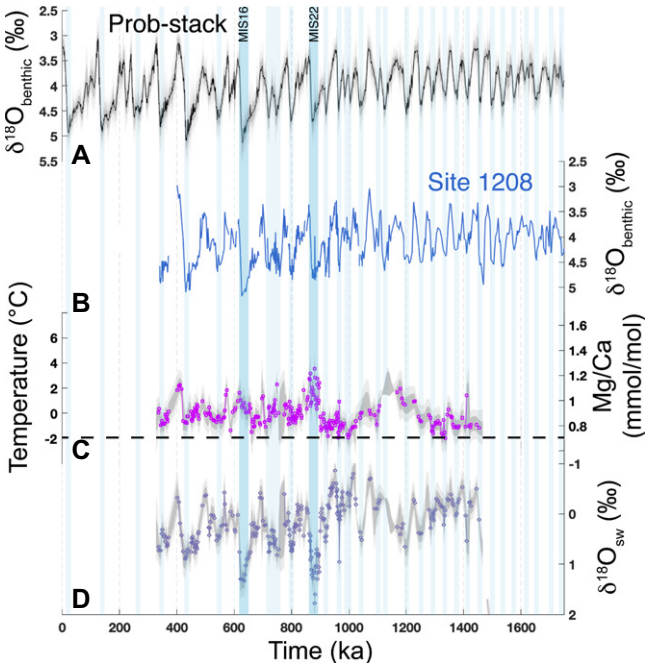

Figure 2. Records from Ocean Drilling Program (ODP) Site 1208, North Pacific. (A) Prob-stack benthic foraminifera $\delta^{18}O$ ($\delta^{18}O_{benthic}$) (Ahn et al., 2017) (black). (B) *Uvigerina* spp. $\delta^{18}O_{benthic}$ (blue). (C) Bottom-water temperature derived from *Uvigerina* spp. Mg/Ca (pink). (D) Seawater $\delta^{18}O$ ($\delta^{18}O_{sw}$) (purple). Sedimentation rate for Site 1208 is 6.5 ± 3.1 cm/k.y. Black dashed line is plotted at –2 °C, which is freezing temperature of seawater. Error envelopes: dark gray, 1σ; light gray, 2σ. MIS—Marine Isotope Stage.

[1]GSA Data Repository item 2020037, appendix and data set, is available online at http://www.geosociety.org/datarepository/2020/, or on request from editing@geosociety.org.

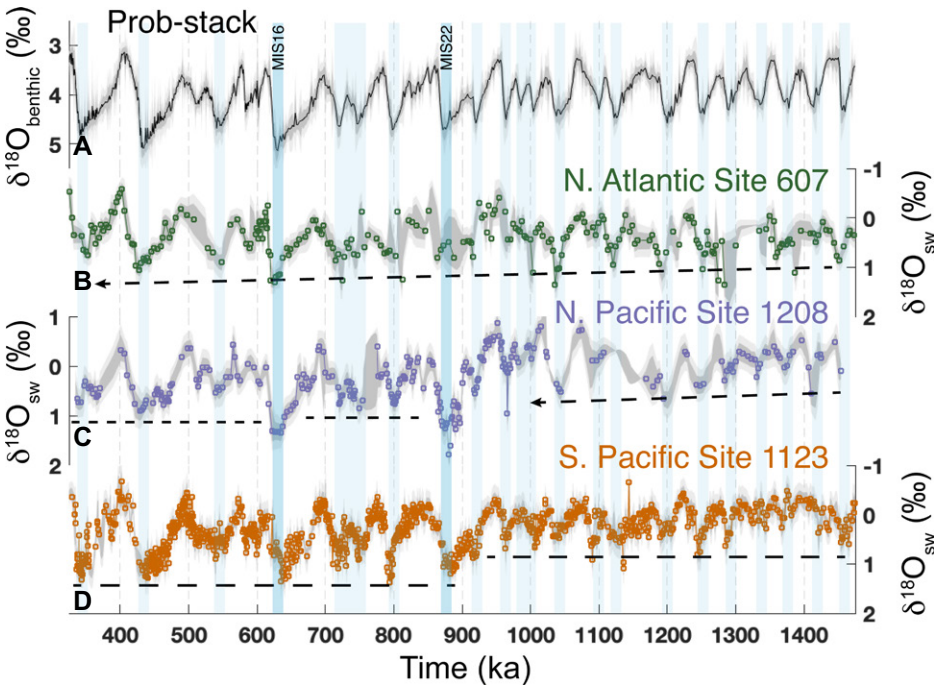

Figure 3. (A) Prob-stack benthic foraminifera $\delta^{18}O$ ($\delta^{18}O_{benthic}$) (Ahn et al., 2017). (B–D) Seawater $\delta^{18}O$ ($\delta^{18}O_{sw}$) records from: (B) Deep Sea Drilling Project (DSDP) Site 607, North Atlantic (*Uvigerina* spp., *Cibicidoides wuellerstorfi*, *Oridorsalis umbonatus*) (Sosdian and Rosenthal, 2009; Ford et al., 2016); (C) Ocean Drilling Program (ODP) Site 1208, North Pacific (*Uvigerina* spp.) (this study); and (D) ODP Site 1123, South Pacific (*Uvigerina* spp.) (Elderfield et al., 2012). Error envelopes: dark gray, 1σ; light gray, 2σ. MIS—Marine Isotope Stage.

via brine rejection from sea-ice formation. Additionally, changes in sea ice in the Bering Sea (Stroynowski et al., 2017; Detlef et al., 2018; Kender et al., 2018) show northern high-latitude transformations that may have influenced NCW production in the Atlantic. Although sea-ice formation itself does not appreciably alter the $\delta^{18}O_{sw}$ value (Craig and Gordon, 1965), a salinity increase influences stratification and deep-ocean water mass formation.

These ocean-circulation and deep-ocean water mass formation changes influenced the regional $^{18}O_{sw}$ records at each site. For DSDP Site 607, a $\delta^{18}O_{sw}$ increase may be masked by corrosive, negative-$\delta^{18}O_{sw}$ SCW (LeGrande and Schmidt, 2006) penetrating further into the North Atlantic as shown from the carbonate saturation-state record which suggests that deep-ocean carbon storage increased during glacials after ca. 900 ka (Lear et al., 2016). On the Chatham Rise, ODP Site 1123 is sensitive to changes in water-mass boundary conditions (Shipboard Scientific Party, 1999). A switch to more NCW flowing over Site 1123 after the 900 ka event and later glacials may explain the persistent positive $\delta^{18}O_{sw}$ recorded there. In the North Pacific, Site 1208 has a large $\delta^{18}O_{sw}$ excursion due to warm BWTs during MIS 22 (and MIS 16), possibly related to North Pacific stratification (McClymont et al., 2008; Knudson and Ravelo, 2015). After the 900 ka event, $\delta^{18}O_{sw}$ is more positive during MIS 20 and 18 than prior to the transition, suggesting a modest increase in ice volume, though not to the same magnitude as originally interpreted by Elderfield et al. (2012).

GLOBAL ICE VOLUME AND SEA LEVEL

Records at ODP Sites 1208 and 1123 and DSDP Site 607 each have different $\delta^{18}O_{sw}$ trends (Figs. 3B–3D), making it impossible to interpret them individually as recording purely a global ice volume signal; therefore, we stack these three high-resolution records and create a $\delta^{18}O_{sw}$ stack (Fig. 4C). We interpret the $\delta^{18}O_{sw}$ stack as primarily reflecting global ice volume; this assumes that the hydrographic changes are "averaged out" and that changes in atmospheric circulation (McClymont and Rosell-Melé, 2005) and ice sheet $\delta^{18}O$ composition (Winnick and Caves, 2015) do not alter the overall $\delta^{18}O_{sw}$ composition in deep-ocean water mass formation regions. Although other $\delta^{18}O_{sw}$ records exist, they are discontinuous and do not have good interglacial-glacial resolution, so they are not included here. Similar to early $\delta^{18}O_{benthic}$ stacks over the MPT (e.g., Williams et al., 1988; Raymo et al., 1990; Shackleton et al., 1995), our $\delta^{18}O_{sw}$ stack has its limitations (i.e., spatial coverage), and additional records will improve interpretation robustness (i.e., Lisiecki and Raymo, 2005; Ahn et al., 2017).

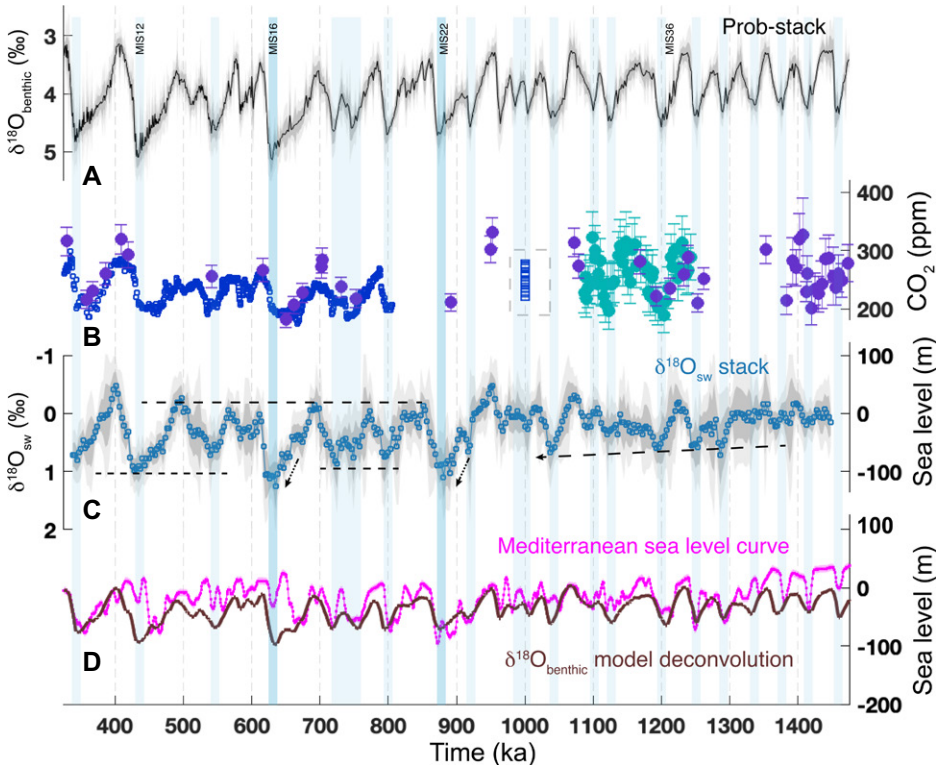

Figure 4. (A) Prob-stack benthic foraminifera $\delta^{18}O$ ($\delta^{18}O_{benthic}$) (Ahn et al., 2017). (B) pCO_2 records (small blue squares: Lüthi et al., 2008; large blue squares: Higgins et al., 2015; purple circles: Hönisch et al., 2009; teal circles: Chalk et al., 2017). (C) Our seawater $\delta^{18}O$ ($\delta^{18}O_{sw}$) stack from Ocean Drilling Program (ODP) Site 1208 (North Pacific) annotated with broad $\delta^{18}O_{sw}$ changes over the mid-Pleistocene transition (MPT). Error envelopes: dark gray, 1σ; light gray, 2σ. (D) Sea-level curves (De Boer et al., 2010; Rohling et al., 2014). MIS—Marine Isotope Stage.

The $\delta^{18}O_{sw}$ stack shows gradual and abrupt increases in ice volume over the MPT. Through the early Pleistocene, there was a gradual increase in ice volume (Fig. 4C). At MIS 22, there was an abrupt increase in ice volume, likely in Antarctica due to the transition from land-based to marine-based ice sheets. At MIS 16, there was another large increase in ice volume, likely in the Northern Hemisphere as evidenced by the first appearance of ice-rafted debris from the Laurentide Ice Sheet via the Hudson Strait (Hodell et al., 2008).

If we use the relationship that a 0.1‰ change in $\delta^{18}O_{sw}$ equals a 10 m change in sea level (Fairbanks, 1989), this equates to an ~45 m additional drop in sea level over the MPT (calculated as the sea-level change from MIS 36 to MIS 12; Fig. 4C). MISs 21–13 are "weak" interglacials consistent with the lower pCO_2 values (Fig. 4B) measured in ice cores (Lüthi et al., 2008) and boron isotope proxies (Hönisch et al., 2009; Chalk et al., 2017). Sea-level estimates from the $\delta^{18}O_{sw}$ stack (Fig. 4C), the Mediterranean sea-level curve of Rohling et al. (2014), and a model deconvolution of $\delta^{18}O_{benthic}$ records (De Boer et al., 2010) (Fig. 4D) have similar amplitude and basic structure over the MPT, although the timing and intensity of sea-level change differs between records. For instance, MIS 16 does not appear as a large glacial in the Mediterranean sea-level curve but does in our $\delta^{18}O_{sw}$ stack and the $\delta^{18}O_{benthic}$ deconvolution. These differences are probably largely attributable to the different assumptions entailed by these various methods of reconstructing past sea level.

DEVELOPMENT OF THE 100 K.Y. CYCLE

The 100 k.y. cycle gains statistical significance at MIS 22 and dominates the spectral signal in a diverse set of records by MIS 16 (Clark et al., 2006; McClymont et al., 2013); both of these intervals are associated with large changes in our $\delta^{18}O_{sw}$ stack and thus ice volume. Wavelet analysis of the $\delta^{18}O_{sw}$ stack shows a similar pattern (see the Data Repository). Mechanistically, what caused the sensitivity of the climate system to the 100 k.y. eccentricity cycle to change? It was likely some combination of atmospheric CO_2 drawdown and change in ice sheet dynamics (Raymo et al., 1997; Tabor and Poulsen, 2016; Farmer et al., 2019; Willeit et al., 2019). At MIS 22, ocean carbon storage increased (Lear et al., 2016; Farmer et al., 2019) and deep-ocean circulation reorganized (Pena and Goldstein, 2014). Additionally, the modest increase in Antarctic ice volume shown in our $\delta^{18}O_{sw}$ stack and the hypothesized transition to fully marine-based ice sheet margins (Raymo et al., 2006) may have initiated sensitivity to the 100 k.y. cycle. The growth of large Northern Hemisphere ice sheets at MIS 16 (Hodell et al., 2008) may have been supported by regolith removal (Clark and Pollard, 1998) and strengthened the 100 k.y. cycle.

ACKNOWLEDGMENTS

This work greatly benefited from discussions with K. Thirumalai, Y. Rosenthal, S. Crowhurst, J. Farmer, L. Haynes, D. Hodell, B. Hönisch, S. Woodard, and three anonymous reviewers. We thank E. Arnold, P. Rumford, and the International Ocean Discovery Program core repository for providing samples. We are grateful to C. Chang, A. Dial, K. Esswein, M. Greaves, W. Huang, B. Lindsey, A. Piotrowski, and S. Severmann for laboratory support. This research used the Queen Mary University of London (QMUL) Apocrita high-performance computing facility, supported by the QMUL IT Services Research group. This work was funded by the U.S. National Science Foundation (OCE-1436014; HLF and MER) with support from the Natural Environment Research Council (NE/N015045/1; HLF), Lamont Climate Center (HLF), and the Vetlesen Foundation (MER).

REFERENCES CITED

Ahn, S., Khider, D., Lisiecki, L.E., and Lawrence, C.E., 2017, A probabilistic Pliocene–Pleistocene stack of benthic $\delta^{18}O$ using a profile hidden Markov model: Dynamics and Statistics of the Climate System, v. 2, p. 91–116, https://doi.org/10.1093/climsys/dzx002.

Brennan, C.E., Meissner, K.J., Eby, M., Hillaire-Marcel, C., and Weaver, A.J., 2013, Impact of sea ice variability on the oxygen isotope content of seawater under glacial and interglacial conditions: Paleoceanography, v. 28, p. 388–400, https://doi.org/10.1002/palo.20036.

Butcher, S., King, T., and Zalewski, L., 2017, Apocrita—High Performance Computing Cluster for Queen Mary University of London: London, Queen Mary University of London Technical Report, 2 p., https://doi.org/10.5281/zenodo.438045.

Chalk, T.B., et al., 2017, Causes of ice age intensification across the Mid-Pleistocene Transition: Proceedings of the National Academy of Sciences of the United States of America, v. 114, p. 13,114–13,119, https://doi.org/10.1073/pnas.1702143114.

Clark, P.U., and Pollard, D., 1998, Origin of the Middle Pleistocene Transition by ice sheet erosion of regolith: Paleoceanography, v. 13, p. 1–9, https://doi.org/10.1029/97PA02660.

Clark, P.U., Archer, D., Pollard, D., Blum, J.D., Rial, J.A., Brovkin, V., Mix, A.C., Pisias, N.G., and Roy, M., 2006, The middle Pleistocene transition: Characteristics, mechanisms, and implications for long-term changes in atmospheric pCO_2: Quaternary Science Reviews, v. 25, p. 3150–3184, https://doi.org/10.1016/j.quascirev.2006.07.008.

Craig, H., and Gordon, L.I., 1965, Deuterium and oxygen-18 variations in the ocean and the marine atmosphere, *in* Tongiorgi, E., ed., Stable Isotopes in Oceanographic Studies and Paleotemperatures: Pisa, Consiglio Nazionale delle Ricerche, Laboratorio di Geologia Nucleare, p. 9–130.

De Boer, B., van de Wal, R.S.W., Bintanja, R., Lourens, L.J., and Tuenter, E., 2010, Cenozoic global ice-volume and temperature simulations with 1-D ice-sheet models forced by benthic $\delta^{18}O$ records: Annals of Glaciology, v. 51, p. 23–33, https://doi.org/10.3189/172756410791392736.

Detlef, H., Belt, S.T., Sosdian, S.M., Smik, L., Lear, C.H., Hall, I.R., Cabedo-Sanz, P., Husum, K., and Kender, S., 2018, Sea ice dynamics across the Mid-Pleistocene transition in the Bering Sea: Nature Communications, v. 9, 941, https://doi.org/10.1038/s41467-018-02845-5.

Elderfield, H., Greaves, M., Barker, S., Hall, I.R., Tripati, A., Ferretti, P., Crowhurst, S., Booth, L., and Daunt, C., 2010, A record of bottom water temperature and seawater $\delta^{18}O$ for the Southern Ocean over the past 440 kyr based on Mg/Ca of benthic foraminiferal *Uvigerina* spp.: Quaternary Science Reviews, v. 29, p. 160–169, https://doi.org/10.1016/j.quascirev.2009.07.013.

Elderfield, H., Ferretti, P., Greaves, M., Crowhurst, S., McCave, I.N., Hodell, D., and Piotrowski, A.M., 2012, Evolution of ocean temperature and ice volume through the Mid-Pleistocene Climate Transition: Science, v. 337, p. 704–709, https://doi.org/10.1126/science.1221294.

Fairbanks, R.G., 1989, A 17,000-year glacio-eustatic sea level record: Influence of glacial melting rates on the Younger Dryas event and deep-ocean circulation: Nature, v. 342, p. 637–642, https://doi.org/10.1038/342637a0.

Farmer, J.R., et al., 2019, Deep Atlantic Ocean carbon storage and the rise of 100,000-year glacial cycles: Nature Geoscience, v. 12, p. 355–360, https://doi.org/10.1038/s41561-019-0334-6.

Ford, H.L., Sosdian, S.M., Rosenthal, Y., and Raymo, M.E., 2016, Gradual and abrupt changes during the Mid-Pleistocene Transition: Quaternary Science Reviews, v. 148, p. 222–233, https://doi.org/10.1016/j.quascirev.2016.07.005.

Higgins, J.A., Kurbatov, A.V., Spaulding, N.E., Brook, E., Introne, D.S., Chimiak, L.M., Yan, Y., Mayewski, P.A., and Bender, M.L., 2015, Atmospheric composition 1 million years ago from blue ice in the Allan Hills, Antarctica: Proceedings of the National Academy of Sciences of the United States of America, v. 112, p. 6887–6891, https://doi.org/10.1073/pnas.1420232112.

Hodell, D.A., Channell, J.E.T., Curtis, J.H., Romero, O.E., and Röhl, U., 2008, Onset of "Hudson Strait" Heinrich events in the eastern North Atlantic at the end of the middle Pleistocene transition (~640 ka)?: Paleoceanography, v. 23, PA4218, https://doi.org/10.1029/2008PA001591.

Hönisch, B., Hemming, N.G., Archer, D., Siddall, M., and McManus, J.F., 2009, Atmospheric carbon dioxide concentration across the mid-Pleistocene transition: Science, v. 324, p. 1551–1554, https://doi.org/10.1126/science.1171477.

Kemp, A.E.S., Grigorov, I., Pearce, R.B., and Naviera Garabato, A.C., 2010, Migration of the Antarctic Polar Front through the mid-Pleistocene transition: Evidence and climatic implications: Quaternary Science Reviews, v. 29, p. 1993–2009, https://doi.org/10.1016/j.quascirev.2010.04.027.

Kender, S., et al., 2018, Closure of the Bering Strait caused Mid-Pleistocene Transition cooling: Nature Communications, v. 9, 5386, https://doi.org/10.1038/s41467-018-07828-0.

Knudson, K.P., and Ravelo, A.C., 2015, North Pacific Intermediate Water circulation enhanced by the closure of the Bering Strait: Paleoceanography, v. 30, p. 1287–1304, https://doi.org/10.1002/2015PA002840.

Lear, C.H., Billups, K., Rickaby, R.E.M., Diester-Haass, L., Mawbey, E.M., and Sosdian, S.M., 2016, Breathing more deeply: Deep ocean carbon storage during the mid-Pleistocene climate transition: Geology, v. 44, p. 1035–1038, https://doi.org/10.1130/G38636.1.

LeGrande, A.N., and Schmidt, G.A., 2006, Global gridded data set of the oxygen isotopic composition in seawater: Geophysical Research Letters, v. 33, L12604, https://doi.org/10.1029/2006GL026011.

Lin, L., Khider, D., Lisiecki, L.E., and Lawrence, C.E., 2014, Probabilistic sequence alignment of stratigraphic records: Paleoceanography, v. 29, p. 976–989, https://doi.org/10.1002/2014PA002713.

Lisiecki, L.E., 2014, Atlantic overturning responses to obliquity and precession over the last 3 Myr: Paleoceanography, v. 29, p. 71–86, https://doi.org/10.1002/2013PA002505.

Lisiecki, L.E., and Raymo, M.E., 2005, A Pliocene-Pleistocene stack of 57 globally distributed benthic $\delta^{18}O$ records: Paleoceanography, v. 20, PA1003, https://doi.org/10.1029/2004PA001071.

Lüthi, D., et al., 2008, High-resolution carbon dioxide concentration record 650,000–800,000 years before present: Nature, v. 453, p. 379–382, https://doi.org/10.1038/nature06949.

McClymont, E.L., and Rosell-Melé, A., 2005, Links between the onset of modern Walker circulation and the mid-Pleistocene climate transition: Geology, v. 33, p. 389–392, https://doi.org/10.1130/G21292.1.

McClymont, E.L., Rosell-Melé, A., Haug, G.H., and Lloyd, J.M., 2008, Expansion of subarctic water masses in the North Atlantic and Pacific oceans and implications for mid-Pleistocene ice sheet growth: Paleoceanography, v. 23, PA4214, https://doi.org/10.1029/2008PA001622.

McClymont, E.L., Sosdian, S.M., Rosell-Melé, A., and Rosenthal, Y., 2013, Pleistocene sea-surface temperature evolution: Early cooling, delayed glacial intensification, and implications for the mid-Pleistocene climate transition: Earth-Science Reviews, v. 123, p. 173–193, https://doi.org/10.1016/j.earscirev.2013.04.006.

Morales Maqueda, M.A., Willmott, A.J., and Biggs, N.R.T., 2004, Polynya dynamics: A review of observations and modeling: Reviews of Geophysics, v. 42, RG1004, https://doi.org/10.1029/2002RG000116.

Mudelsee, M., and Schulz, M., 1997, The Mid-Pleistocene climate transition: Onset of 100 ka cycle lags ice volume build-up by 280 ka: Earth and Planetary Science Letters, v. 151, p. 117–123, https://doi.org/10.1016/S0012-821X(97)00114-3.

Pena, L.D., and Goldstein, S.L., 2014, Thermohaline circulation crisis and impacts during the mid-Pleistocene transition: Science, v. 345, p. 318–322, https://doi.org/10.1126/science.1249770.

Raymo, M.E., and Nisancioglu, K.H., 2003, The 41 kyr world: Milankovitch's other unsolved mystery: Paleoceanography, v. 18, 1011, https://doi.org/10.1029/2002PA000791.

Raymo, M.E., Ruddiman, W.F., Shackleton, N.J., and Oppo, D.W., 1990, Evolution of Atlantic-Pacific $\delta^{13}C$ gradients over the last 2.5 m.y.: Earth and Planetary Science Letters, v. 97, p. 353–368, https://doi.org/10.1016/0012-821X(90)90051-X.

Raymo, M.E., Oppo, D.W., and Curry, W., 1997, The mid-Pleistocene climate transition: A deep sea carbon isotopic perspective: Paleoceanography, v. 12, p. 546–559, https://doi.org/10.1029/97PA01019.

Raymo, M.E., Lisiecki, L.E., and Nisancioglu, K.H., 2006, Plio-Pleistocene ice volume, Antarctic climate, and the global $\delta^{18}O$ record: Science, v. 313, p. 492–495, https://doi.org/10.1126/science.1123296.

Rohling, E.J., Foster, G.L., Grant, K.M., Marino, G., Roberts, A.P., Tamisiea, M.E., and Williams, F., 2014, Sea-level and deep-sea-temperature variability over the past 5.3 million years: Nature, v. 508, p. 477–482, https://doi.org/10.1038/nature13230.

Ruddiman, W.F., Raymo, M.E., Martinson, D.G., Clement, B.M., and Backman, J., 1989, Pleistocene evolution: Northern hemisphere ice sheets and North Atlantic Ocean: Paleoceanography, v. 4, p. 353–412, https://doi.org/10.1029/PA004i004p00353.

Shackleton, N.J., and Opdyke, N.D., 1976, Oxygen-isotope and paleomagnetic stratigraphy of Pacific core V28-239 late Pliocene to latest Pleistocene, *in* Cune, R.M., and Hays, J.D., eds., Investigation of Late Quaternary Paleoceanography and Paleoclimatology: Geological Society of America Memoir 145, p. 449–464, https://doi.org/10.1130/MEM145-p449.

Shackleton, N.J., Crowhurst, S., Hagelberg, T., Pisias, N.G., and Schneider, D.A., 1995, A new late Neogene time scale: Application to Leg 138 sites, *in* Pisias, N.G., et al., eds., Proceedings of the Ocean Drilling Program, Scientific Results, Volume 138, p. 73–101, https://doi.org/10.2973/odp.proc.sr.138.106.1995.

Shipboard Scientific Party, 1999, Leg 181 summary: Southwest Pacific paleoceanography, *in* Carter, R.M., et al., Proceedings of the Ocean Drilling Program, Initial Reports, Volume 181: College Station, Texas, Ocean Drilling Program, p. 1–80, https://doi.org/10.2973/odp.proc.ir.181.101.2000.

Sosdian, S., and Rosenthal, Y., 2009, Deep-sea temperature and ice volume changes across the Pliocene-Pleistocene climate transitions: Science, v. 325, p. 306–310, https://doi.org/10.1126/science.1169938.

Stroynowski, Z., Abrantes, F., and Bruno, E., 2017, The response of the Bering Sea Gateway during the Mid-Pleistocene Transition: Palaeogeography, Palaeoclimatology, Palaeoecology, v. 485, p. 974–985, https://doi.org/10.1016/j.palaeo.2017.08.023.

Tabor, C.R., and Poulsen, C.J., 2016, Simulating the mid-Pleistocene transition through regolith removal: Earth and Planetary Science Letters, v. 434, p. 231–240, https://doi.org/10.1016/j.epsl.2015.11.034.

Talley, L.D., 2013, Closure of the global overturning circulation through the Indian, Pacific, and Southern Oceans: Schematics and transports: Oceanography (Washington, D.C.), v. 26, p. 80–97, https://doi.org/10.5670/oceanog.2013.07.

Thirumalai, K., Quinn, T.M., and Marino, G., 2016, Constraining past seawater $\delta^{18}O$ and temperature records developed from foraminiferal geochemistry: Paleoceanography, v. 31, p. 1409–1422, https://doi.org/10.1002/2016PA002970.

Venz, K.A., Hodell, D.A., Stanton, C., and Warnke, D.A., 1999, A 1.0 Myr record of Glacial North Atlantic Intermediate Water variability from ODP site 982 in the northeast Atlantic: Paleoceanography, v. 14, p. 42–52, https://doi.org/10.1029/1998PA900013.

Willeit, M., Ganopolski, A., Calov, R., and Brovkin, V., 2019, Mid-Pleistocene transition in glacial cycles explained by declining CO_2 and regolith removal: Science Advances, v. 5, eaav7337, https://doi.org/10.1126/sciadv.aav7337.

Williams, D.F., Thunell, R.C., Tappa, E., Rio, D., and Raffi, I., 1988, Chronology of the Pleistocene oxygen isotope record: 0–1.88 m.y. B.P.: Palaeogeography, Palaeoclimatology, Palaeoecology, v. 64, p. 221–240, https://doi.org/10.1016/0031-0182(88)90008-9.

Winnick, M.J., and Caves, J.K., 2015, Oxygen isotope mass-balance constraints on Pliocene sea level and East Antarctic Ice Sheet stability: Geology, v. 43, p. 879–882, https://doi.org/10.1130/G36999.1.

Worthington, L.V., 1981, The water masses of the world ocean: Some results of a fine-scale census, *in* Warren, B.A., and Wunsch, C., eds., Evolution of Physical Oceanography, Chapter 2: Cambridge, Massachusetts, MIT Press, p. 42–69.

Printed in USA